Membrane-Associated Ubiquitin Ligase RNF152 Orchestrates Melanogenesis via Tyrosinase Ubiquitination

Ryota Ueda [1], Rina Hashimoto [1], Yuki Fujii [1], José C.J.M.D.S. Menezes [1], Hirotaka Takahashi [2], Hiroyuki Takeda [2], Tatsuya Sawasaki [2], Tomonori Motokawa [3], Kenzo Tokunaga [4,*] and Hideaki Fujita [1,*]

[1] Faculty of Pharmaceutical Sciences, Nagasaki International University, Nagasaki, Japan
[2] Proteo-Science Center, Ehime University, Ehime, Japan
[3] Frontier Research Center, POLA Chemical Industries, Inc., Tokyo, Japan
[4] Department of Pathology, National Institute of Infectious Diseases, Tokyo, Japan
* Correspondence: tokunaga@nih.go.jp (K.T.); fujita@niu.ac.jp (H.F.);
  Tel: +81-3-5285-1111 (K.T.); +81-956-20-5638 (H.F.)

Abstract: Lysosomal degradation of tyrosinase, a pivotal enzyme in melanin synthesis, negatively impacts melanogenesis in melanocytes. Nevertheless, the precise molecular mechanisms by which lysosomes target tyrosinase have remained elusive. Here, we identify RING finger protein 152 (RNF152) as a membrane-associated ubiquitin ligase specifically targeting tyrosinase for the first time, utilizing AlphaScreen technology. We observed that modulating RNF152 levels in B16 traffi cells, either via overexpression or siRNA knockdown, resulted in decreased or increased tyrosinase levels, respectively. Notably, RNF152 and tyrosinase colocalized at the trans-Golgi network (TGN). However, upon treatment with lysosomal inhibitors, both proteins appeared in the lysosomes, indicating that tyrosinase undergoes RNF152-mediated lysosomal degradation. Through ubiquitination assays, we found the indispensable roles of both the RING and transmembrane (TM) domains of RNF152 in facilitating tyrosinase ubiquitination. In summary, our findings underscore RNF152 as a tyrosinase-specific ubiquitin ligase essential for regulating melanogenesis in melanocytes.

Keywords: lysosome; melanogenesis; melanosome; RNF152; tyrosinase; ubiquitin ligase

1. Introduction

The abundance of membrane proteins directly correlates with their activity and physiological functions in eukaryotic cells. Precise regulation of membrane protein turnover, through either proteasomal or lysosomal degradation, is therefore a crucial process [1,2]. Ubiquitination of membrane proteins serves as a targeting signal for either proteasomes or lysosomes, contingent upon the site of occurrence. When ubiquitination of membrane proteins occurs in the endoplasmic reticulum (ER), these proteins are extracted from the ER membrane to the cytosol, where they undergo proteasomal degradation. This pathway, known as ER-associated degradation (ERAD), provides a mechanism for protein quality control at the ER level [3].

The ERAD pathway involves specific membrane-associated ubiquitin ligases (*e.g.*, Hrd1, MARCH6) localized in the ER. Conversely, when ubiquitination of membrane proteins occurs in post-Golgi compartments such as the plasma membrane, trans-Golgi network (TGN), or endosomes, the ubiquitinated proteins are targeted to late endosomes (LEs)/multivesicular bodies (MVBs) and sorted into intraluminal vesicles of MVBs where they undergo degradation through MVBs-lysosome fusion [4,5]. Multiple ubiquitin ligases participate in the ubiquitin-dependent control of endocytosis and lysosomal degradation of membrane proteins [6].

Numerous soluble cytosolic ubiquitin ligases (e.g., Nedd4-1, WWP1, WWP2, SMURF1, SMURF2, Cbl) directly or indirectly recognize their specific substrate membrane proteins and facilitate their

ubiquitination. Membrane-associated ubiquitin ligases, including most of the MARCH family and some members of the RNF family, are localized in specific compartments of the secretory/endocytic system, where their substrate membrane proteins are also localized. MARCH1, -2, -3, and -8 are localized in endosomes and/or lysosomes, and ubiquitinate their respective substrates [7–10].

RNF152, a membrane-associated RING (really interesting new gene)-finger ubiquitin ligase, is localized in lysosomes and reportedly plays a role in lysosome-related apoptosis [11]. RNF152 also acts as a negative regulator of the mTORC1 pathway by targeting RagA for K63-linked ubiquitination and subsequent proteasomal degradation [12]. RNF152, along with RNF182, RBF183, RNF186, constitutes RNF183 family, consisting of closely related genes encoding a RING-finger domain (C3HC4) at their N-terminus and one or two predicted transmembrane domains at their C-terminus with high homology [13].

The abundance of tyrosinase, a key enzyme in melanin synthesis, directly affects melanogenesis (cell pigmentation level). Tyrosinase is translated in the ER as a type I membrane glycoprotein, trafficked via the Golgi, and delivered to melanosomes, where melanin is synthesized and accumulated [14–19]. Certain whitening reagents reduce the protein level of tyrosinase without altering its transcription level [20], often resulting in the degradation of tyrosinase through proteasomal or lysosomal activity. Linoleic acid induces proteasomal degradation of tyrosinase, presumably via the ERAD pathway [21,22], while phenylthiourea (PTU) [23] and inulavosin [24,25] induce lysosomal degradation of tyrosinase. The mechanisms by which these reagents differentially channel tyrosinase to these two degradation pathways remain unclear. Elucidating the processes through which cells or whitening reagents regulate melanogenesis will necessitate the identification and characterization of tyrosinase-specific ubiquitin ligases. In this study, employing AlphaScreen technology, we identified RNF152 as a membrane-associated ubiquitin ligase that specifically targets tyrosinase for ubiquitination. Our findings reveal that this ubiquitin ligase directs tyrosinase toward lysosomal degradation, ultimately regulating melanogenesis.

2. Experimental Procedures

2.1. Antibodies and Reagents

Rabbit polyclonal antibodies against mouse tyrosinase and Tyrp-1 were described previously [24,26]. Rabbit polyclonal antibody against synthetic peptide of mouse RNF152 (G_{145}APPEA VEEEPDRRGV VK$_{162}$) was obtained from Sigma-Aldrich (St. Louis, MO, USA) and evaluated (Supplementary Figure S1). The mouse monoclonal antibody against human Lamp-1 (1D4B) was generously provided by Dr. K. Furuta (National Cancer Center Research Institute, Tokyo, Japan). Mouse monoclonal antibodies against β-actin and c-myc, and rabbit antibodies against HA and c-myc were purchased from Sigma-Aldrich. The goat antibody against HA was from GenScript (Piscataway, NJ, USA). The mouse anti-ubiquitin monoclonal antibody (FK2) was from Nippon Bio-Test Laboratories (Tokyo). All secondary antibodies for immunofluorescence analysis were purchased from Molecular Probes (Eugene, OR, USA). The protease inhibitor cocktail was from Nacalai Tesque (Kyoto, Japan). *N*-ethylmaleimide was from Sigma-Aldrich. Pepstatin A, leupeptin, and E64d were from Peptide Institute (Osaka, Japan). Bafilomycin A1 was from BioViotica (San Diego, CA, USA). Protein A-coupled Sepharose 4B was from GE Healthcare UK (Buckinghamshire, UK).

2.2. Cell Culture

Mouse melanoma B16, HEK293T and HeLa cells were obtained from JCRB Cell Bank (Japan). Mouse melanoma B16 cells were cultured in MEM supplemented with 10% FBS. HEK293T and HeLa cells were cultured in DMEM supplemented with 10% FBS. All cells were maintained at 37 °C in humidified 5% CO_2 atmosphere.

2.3. Screening for E3 Ubiquitin Ligases that Interact with Tyrosinase

A protein array containing 224 biotinylated human and mouse E3 ligases was constructed using a wheat germ cell-free synthesis system [27,28]. V5 epitope-tagged tyrosinase and dihydrofolate

reductase (DHFR) were synthesized with this system. Binding of V5-tagged tyrosinase to the protein array was assayed by AlphaScreen technology with slight modification from previous protocols [29]. In summary, 1 µL of the cell-free synthesized V5-tagged bait protein and 1 µL of biotinylated E3 protein were mixed in a 15 µL AlphaScreen buffer containing 100 mM Tris-HCl (pH 8.0), 0.01% Tween 20, 100 mM NaCl, and 1 mg/mL BSA in an OptiPlate 384 titer plate (PerkinElmer; Waltham, MA, USA). This protein mixture was incubated for 1 h at 26 °C, followed by the addition of a 10 µL detection mixture (0.01 µL anti-V5 antibody (Invitrogen; Carlsbad, CA, USA), 0.1 µL streptavidin-conjugated AlphaScreen donor beads, and 0.1 µL protein A-conjugated AlphaScreen acceptor beads in AlphaScreen buffer), and incubated for another 1 h at 26 °C. AlphaScreen luminescent signal was measured by EnVision multilabel plate reader (PerkinElmer), and relative luminescent signal was calculated by dividing the value obtained from the interaction between the E3 ligase and tyrosinase by that obtained from the E3 ligase and DHFR interaction.

2.4. Plasmid Construction and Transfection, siRNA and Transfection

The cDNAs encoding human RNF152 or mouse tyrosinase and mouse Tyrp-1 were PCR-amplified and subcloned into either pcDNA3.1/Myc-His(-) B (Invitrogen) or pCMV-HA-C (Clontech; Palo Alto, CA, USA). The primer sets used were as follows: RNF152 (5'- ATA GAATTC ATG GAG ACG CTG TCC CAG GAC TCT CTG C -3', 5'- ATA GGATCC GCC ACA GGA TAT CAC AGT GAA GCG CTT AG -3'); mouse tyrosinase (5'- ATA GAATTC ATG TTC TTG GCT GTT TTG TAT TGC CTT CTG TGG -3', 5'- ATA GTCGAC G CAG ATG GCT CTG ATA CAG CAA GCT GTG GTA GTC G -3'), mouse Tyrp-1 (5'-ATA GAATTC ATG AAA TCT TAC AAC GTC CTC CCC CTA GCC-3', 5'-ATA GTCGAC G GAC CAT GGA GTG GTT AGG ATT CGG GAG CTC -3'). Two mutant RNF152-myc plasmids were obtained from GenScript (Tokyo, Japan). The 3xFLAG-ubiquitin plasmid was described previously [8]. siRNAs, ON-TARGETplus Mouse RNF152 siRNA and ON-TARGETplus Non-targeting Control siRNAs were purchased from Horizon Discovery (Tokyo, Japan). For transfection in B16 cells, TransFast (Roche Molecular Biochemicals; Indianapolis, IN, USA) was used as per the manufacturer's instructions. For transfection in HeLa cells, FuGENE 6 (Roche Molecular Biochemicals; Indianapolis, IN, USA) was employed following the manufacturer's instructions. For B16 cell siRNA transfection, RNAiMAX (Thermo Fisher Scientific; Waltham, MA, USA) was used as per the manufacturer's instructions.

2.5. Melanin Content Measurement

The melanin content was measured using the method described by Kim et al. [30] with slight modification. Cultured cells were directly solubilized with 1 M NaOH and boiled at 80 °C for 30 min. The dissolved melanin content was then measured using spectrophotometry at OD_{405}. The values were normalized to the protein concentration and presented as percentages relative to the control.

2.6. IP and Western Blotting

Total cell lysates and immunoprecipitated proteins were prepared as described previously [8]. Briefly, cells were lysed in TBS-T buffer (50 mM Tris-HCl buffer (pH 7.5), 0.15 M NaCl, 1% Triton X-100, and 0.5% deoxycholic acid) containing a protease inhibitor cocktail and 10 mM *N*-ethylmaleimide. The lysate was centrifuged at 21,500 × *g* for 15 min, and the supernatant was used as the total cell lysate for immunoblotting or IP. Protein A-coupled Sepharose 4B was pre-incubated with appropriate antibodies for 2 hours at 4 °C. The total cell lysate was then incubated with antibody-coupled Sepharose overnight at 4 °C, washed three times with TBS-T buffer. Immunoprecipitated proteins were eluted with SDS sample buffer, subjected to SDS-PAGE, and the immunoreactive bands were visualized using an ECL detection kit (GE Healthcare). The bands were scanned with ChemiDoc system (Bio-Rad, Japan), and band intensities were quantitated with Image J software (NIH, MD, USA).

2.7. Confocal Immunofluorescence Microscopy

B16 and HeLa cells were cultured on coverslips, fixed with 4% paraformaldehyde for 30 min on ice, and permeabilized with 0.05% saponin (Sigma-Aldrich, St. Louis, MO, USA). Fixed cells were subjected to immunofluorescence analysis as described previously [8]. In brief, fixed coverslips were stained with primary antibodies: mouse anti-myc monoclonal antibody (Sigma-Aldrich, St. Louis, MO, USA), and either rabbit anti-tyrosinase or anti-Tyrp-1 antibody. For double staining, secondary antibodies, Alexa 488 donkey anti-mouse IgG (A-21202) and Alexa 568 donkey anti-rabbit IgG (A-10042) were used. Fixed coverslips were also stained with rabbit anti-myc antibody (Sigma-Aldrich), goat anti-HA antibody (GenScript), and either mouse anti-syntaxin 6 (BD Biosciences; London, UK) or anti-Lamp1 antibody. For triple staining, the secondary antibodies used were; Alexa 488 donkey anti-goat IgG (A-11055), Alexa 568 donkey anti-rabbit IgG (A-10422), and Alexa 647 donkey anti-mouse IgG (A-31571). Confocal images were captured using FluoView FV10i (Olympus; Tokyo, Japan) or STELLARIS 5 (Leica Microsystems, Tokyo, Japan).

3. Results

3.1. Tyrosinase Ubiquitination in B16 Melanoma Cells

Detection of protein ubiquitination involves immunoprecipitation (IP) of total ubiquitinated proteins using an anti-ubiquitin antibody, combined with immunoblotting using antibody against the protein of interest [31]. To assess tyrosinase ubiquitination in B16 melanoma cells, we employed anti-ubiquitin antibody along with anti-tyrosinase antibody (Figure 1A). Analysis of cell lysates revealed a robust increase in tyrosinase protein levels in the presence of lysosomal protease inhibitors (LPIs), whereas the levels of Tyrp-1, another melanosome membrane protein, remained unchanged (Figure 1A, Input). This disparity suggests varying turnover rates between these proteins [24]. We observed smear bands representing ubiquitinated tyrosinase along with the normal-sized (76-kDa) tyrosinase in total ubiquitinated proteins when LPIs were present (Figure 1A, IP). As tyrosinase forms homo-oligomers [32], this suggests ubiquitination occurs on a portion of the oligomer subunit. Corresponding experiments using anti-Tyrp-1 antibody did not display smear bands or normal-sized Tyrp-1.
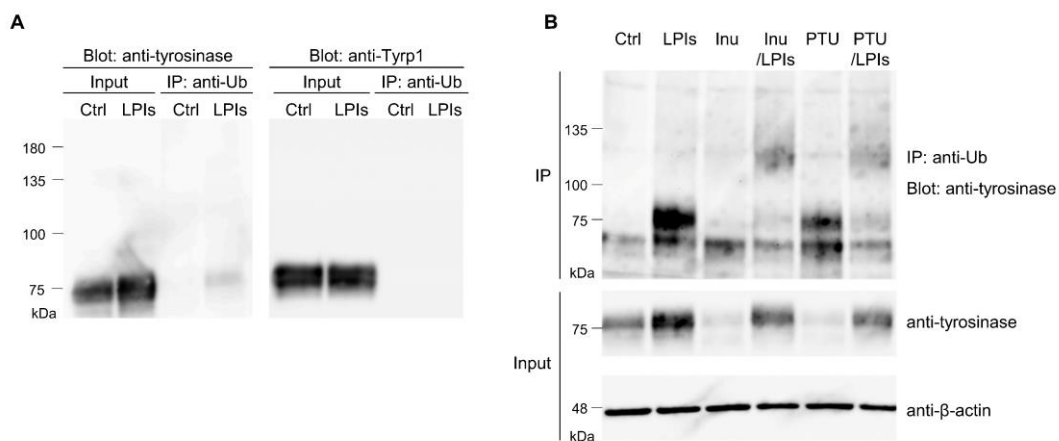
Figure 1. Tyrosinase undergoes ubiquitination and degradation in lysosomes in B16 melanoma cells. (**A**) Cells were treated with either DMSO (control, Ctrl) or LPIs (leupeptin, pepstatin A, E64d; each 40 μM) for 24 h. Lysates were immunoblotted with an anti-tyrosinase or anti-Tyrp-1 antibody. Additionally, lysates were immunoprecipitated with an anti-ubiquitin antibody (IP: anti-Ub) followed by immunoblotting using the anti-tyrosinase or anti-Tyrp-1 antibody. (**B**) Cells were treated with DMSO (control, Ctrl), LPIs, inulavosin (Inu; 15 μM), inulavosin combined with LP (Inu/LP), PTU (PTU; 100 μM), or PTU combined with LP (PTU/LP) for 24 h. Lysates were immunoprecipitated with the anti-ubiquitin antibody followed by immunoblotting with the anti-tyrosinase antibody ("IP: anti-Ub Blot: anti-tyrosinase"), or directly immunoblotted with the anti-tyrosinase or an anti-β-actin antibody.

The impact of inulavosin and PTU on tyrosinase ubiquitination in B16 cells was investigated. Both inulavosin [24] and PTU [23] accelerate tyrosinase degradation rate in lysosomes, and decreased tyrosinase protein levels in our experiments (Figure 1B, anti-tyrosinase in Input, lanes Inu and PTU). However, this degradation was restored in the presence of LPIs (Figure 1B, anti-tyrosinase in Input, lanes Inu/LP and PTU/LPIs). Substantially increased levels of recovered ubiquitinated tyrosinase (smear bands with higher molecular weights) were observed in the presence of inulavosin or PTU combined with LPIs (Figure 1B, lanes Inu/LPIs and PTU/LPIs in IP).

3.2. Identification of Tyrosinase-Specific E3 Ubiquitin Ligase

A screening process was conducted to identify ubiquitin ligases specific for tyrosinase. Using an E3 ubiquitin ligase protein array, we synthesized V5-tagged tyrosinase and DHFR (as negative control) and employed AlphaScreen technology to detect the binding of V5-tyrosinase to the protein array (see Experimental Procedures "Screening for E3 ubiquitin ligases that interact with tyrosinase"). We previously demonstrated that inulavosin interferes directly with copper loading into the luminal domain of tyrosinase, leading to the formation of apo-tyrosinase, and proposed that apo-tyrosinase, possessing certain conformational defect, is selectively delivered to lysosomes [25]. In this study, we performed screenings both in the absence and presence of inulavosin. We assumed that if inulavosin induces conformational change of tyrosinase, it would likely enhance its binding to the ubiquitin ligase in our assay. Out of 67 candidate ligases displaying a relative luminescent signal >15 in the absence of inulavosin, 44 showed higher affinity to V5-tyrosinase in the presence of inulavosin. Among these, RNF152 exhibited the highest affinity for tyrosinase (Table 1), leading to its selection for subsequent analyses.

Table 1. E3 ubiquitin ligases with higher affinity for tyrosinase in the presence of inulavosin.

		E3 binding assay result to V5-Tyrosinase			predicted localization*	predicted number of transmembrane domain*
		Sample/Mock		Inulavosin/DMSO		
Symbol	rank	DMSO	Inulavosin			
RNF152	1	16.65	22.13	1.33	Lysosome	1
VPS41	2	17.99	20.97	1.17	Cytosol, lysosome, Golgi, Endosome	0
RNF41	3	17.84	20.55	1.15	Cytosol	0
ZNF598	4	16.43	18.52	1.13	Cytosol	0
TRIM21	5	19.82	21.73	1.10	Cytosol, Nucleus	0
TRAF7	6	21.32	23.25	1.09	Plasma Membrane	0
TRIM43	7	17.81	19.22	1.08	Cytosol, Nucleus	0
TRIM9	8	23.53	25.33	1.08	Cytoskelton, Cytosol	0
TRAF6	9	24.18	25.91	1.07	Cytosol, Endosome, Nucleous, Plasma Membrane	0
RBX1	10	16.45	17.55	1.07	Cytosol, Nucleus	0
PDZRN3	11	24.01	25.34	1.06	Cytosol, Nucleus	0
RNF144A	12	23.46	24.72	1.05	Golgi, Plasma Membrane	1
LINCR	13	34.53	36.35	1.05	Cytosol	0
TRAF2	14	19.89	20.93	1.05	Cytosol	0
TRIM15	15	26.50	27.84	1.05	Cytosol, Nucleus	0
LNX2	16	16.28	17.02	1.05	Cytosol	0
RNF182	17	19.25	20.09	1.04	Nucleus	0
TRIM10	18	25.40	26.48	1.04	Nucleus	0
ZNRF1	19	18.15	18.85	1.04	Cytosol	0
RBBP6	20	38.17	39.59	1.04	Cytoskelton, Cytosol, Nucleous	0
PEX10	21	22.45	23.28	1.04	Peroxisome	1
TRAF5	22	17.29	17.91	1.04	Cytosol	0
MEX3B	23	31.98	33.10	1.03	Cytosol, Nucleus	0
MIB2	24	33.19	34.32	1.03	Cytosol	0
PCGF1	25	17.95	18.55	1.03	Nucleous	0
RNF38	26	63.97	66.07	1.03	Nucleous	0
RNF6	27	21.45	22.15	1.03	Nucleous	0
RNF125	28	15.06	15.55	1.03	Endopralmic Reticlum, Golgi	0
RNF115	29	36.71	37.90	1.03	Cytosol	0
PPIL2	30	23.45	24.19	1.03	Cytosol	0
RNF126	31	38.46	39.64	1.03	Cytosol, Nucleus	0
TRIM4	32	24.42	25.13	1.03	Cytosol	0
RNF138	33	18.04	18.56	1.03	Nucleous	0
NFXL1	34	25.05	25.74	1.03	Nucleous	0
RNF32	35	47.30	48.52	1.03	Endosome	0

RNF40	36	16.74	17.11	1.02	Endosome	0
RNF12	37	49.34	50.44	1.02	Cytosol, Nucleus	0
MARCH3	38	21.47	21.87	1.02	Endosome, Lysosome	2
RNF180	39	16.33	16.60	1.02	Endopralmic Reticulum, Nucleous	1
RNF8	40	23.01	23.34	1.01	Cytosol, Nucleus	0
RFWD2	41	17.05	17.29	1.01	Cytosol, Nucleus	0
CHFR	42	27.09	27.35	1.01	Nucleous	0
RNF175	43	27.95	28.08	1.00	Endopralmic Reticulum, Golgi	5
ANKIB1	44	28.62	28.64	1.00	Cytosol	0

*Predictions were obtained from the following sites;
GeneCard: https://www.genecards.org
Uniprote: https://www.uniprot.org

3.3. RNF152 Regulates Expression of Tyrosinase in B16 Cells

We next examined the effects of RNF152 expression levels on tyrosinase and melanin content in B16 cells. Cells transfected with myc-tagged mouse RNF152 (RNF152-myc) demonstrated significantly reduced levels of tyrosinase and melanin, but not of Tyrp-1 (Figure 2A,B). It should be noted that exogenously expressed RNF152-myc displayed doublet bands with anti-myc antibody due to an unknown reason [11]. Immunofluorescence analysis of transfected cells exhibited a specific reduction in tyrosinase but not in Tyrp-1 (Figure 2C). Transfecting siRNA specific to mouse RNF152 reduced the expression of endogenous RNF152 and concurrently increased tyrosinase expression (Figure 2D,E). Despite this alteration, we did not observe an increase in melanin content (data not shown), possibly due to the insufficient suppression of RNF152.
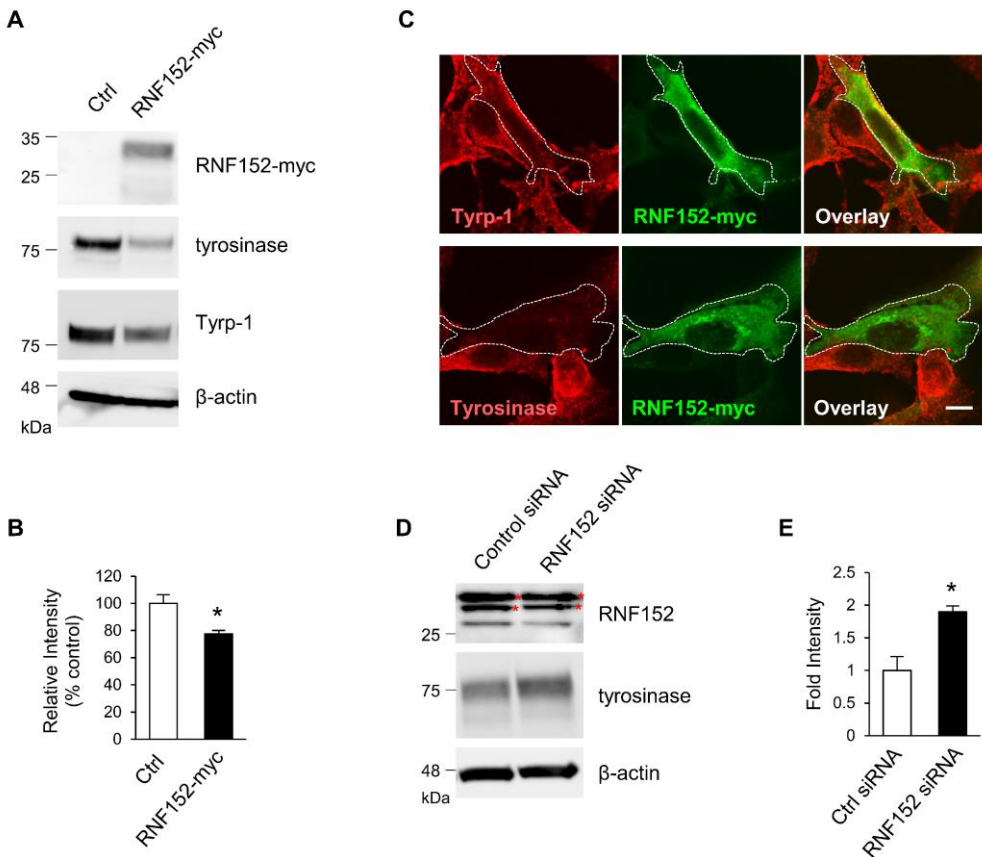
Figure 2. RNF152 modulation influences tyrosinase expression in B16 cells. (**A**) Cells were transfected with either an empty vector (Ctrl) or RNF152-myc. Lysates were immunoblotted with anti-tyrosinase, anti-Tyrp-1, anti-β-actin, and anti-myc antibodies. (**B**) Cells were transfected with either an empty vector (Ctrl) or RNF152-myc, and melanin content was assayed. (*, p< 0.05 vs. control by t-test; n = 3). (**C**) Cells transfected with RNF152-myc were subjected to immunofluorescence analysis with anti-myc, anti-tyrosinase, or anti-Tyrp-1 antibodies. Dotted white lines indicate transfected cells. Scale bar:

10 μm. (**D**) Cells were transfected with either control or RNF152 siRNA. Lysates were immunoblotted with anti-RNF152, anti-tyrosinase, or anti-β-actin antibodies. Red asterisks indicate non-specific bands in the RNF152 blotting (see Figure S1). (**E**) Expression levels of tyrosinase were quantified in the bands. (*, $p < 0.05$ vs. control by t-test; $n = 3$).

3.4. RNF152 Co-Localizes with Tyrosinase in TGN and Degrades it in Lysosomes

To assess the routes of RNF152-induced tyrosinase degradation, HEK293T cells were transfected with HA-tagged mouse tyrosinase (tyrosinase-HA) alone or together with both RNF152-myc and tyrosinase-HA. These cells were treated with bafilomycin A1 (vacuolar H^+-ATPase inhibitor) or LPIs for 14 hours, followed by immunoblotting analysis (Figure 3A). RNF152-myc prompted the degradation of tyrosinase-HA (Figure 3A, anti-HA, compare lane 1 with lane 2), but this degradation was restored in the presence of LPIs and bafilomycin A1 (Figure 3A, anti-HA, compare lane 2 with lanes 3 and 4"). Next, to evaluate the intracellular localization and degradation pathways of tyrosinase and RNF152, HeLa cells transfected with tyrosinase-HA and RNF152-myc were subjected to immunofluorescence analysis following treatment with LPIs and bafilomycin A1 (Figure 3B). Exogenously expressed tyrosinase-HA along with RNF152-myc were localized at a perinuclear region and demonstrated co-localization with syntaxin-6 (TGN marker), while exhibiting no co-localization with Lamp-1 (LEs and lysosome marker) (Figure 3B, Control (DMSO)). In contrast, in the presence of LPIs or bafilomycin A1, their expression levels were elevated, and they were observed within enlarged vesicular structures, demonstrating co-localization with Lamp-1 (Figure 3B, Baf A1 and LPIs).
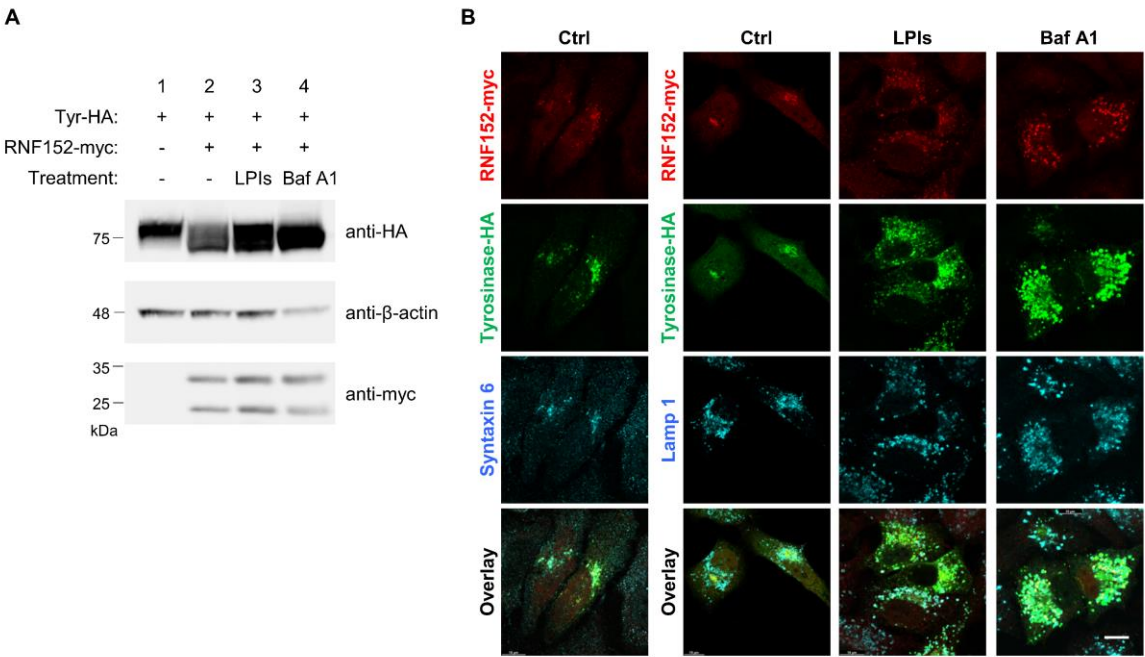
Figure 3. RNF152 is co-localized with tyrosinase-HA in the TGN and degrades it in lysosomes. (**A**) HEK293T cells transfected with tyrosinase-HA (Tyr-HA) alone (lane 1), or RNF152-myc and Tyr-HA in combination (lanes 2, 3, and 4), were treated with DMSO (control; lanes 1 and 2), LPIs (leupeptin, pepstatin A, E64d; each 40 μM; lane 3) or bafilomycin A1 (Baf A1, 5 μM; lane 4)for 14 h. Lysates were immunoblotted with anti-HA, anti-β-actin, or anti-myc antibodies. (**B**) HeLa cells transfected with RNF152-myc and Tyr-HA were treated with DMSO (Ctrl), LPIs or bafilomycin A1 (Baf A1) as in (A), fixed, and subjected to immunofluorescence analysis with anti-myc, anti-HA, anti-syntaxin 6 (TGN marker), or anti-Lamp1 (LEs/lysosome marker) antibodies. Scale bar: 10 μm.

3.5. RNF152 is Associated with Tyrosinase through the Transmembrane (TM) Domain

RNF152 comprises a luminal domain, a single TM domain, and a cytoplasmic region, including a RING domain responsible for ubiquitination activity. To evaluate binding ability and ubiquitination

activity of RNF152 toward tyrosinase, we generated plasmids encoding mutant forms of RNF152: RNF152(C/S) (in which 4 cysteine residues located at the RING domain were replaced by serine) and RNF152(ΔTM) (in which the TM domain located at the C-terminus of RNF152 was deleted). The interaction between RNF152 and tyrosinase was assessed by co-IP analysis in HEK293T cells cotransfected with plasmids encoding tyrosinase-HA and either wild-type (WT) or mutant RNF152-myc. Cell lysate blotting revealed two bands for WT and the C/S mutant, and a single band for the ΔTM mutant (Figure 4, anti-myc in Input) consistent with reported [11]. Co-IP analysis revealed that both WT and C/S mutant were co-immunoprecipitated with tyrosinase-HA, whereas ΔTM mutant displayed no tyrosinase binding ability (Figure 4, IP).
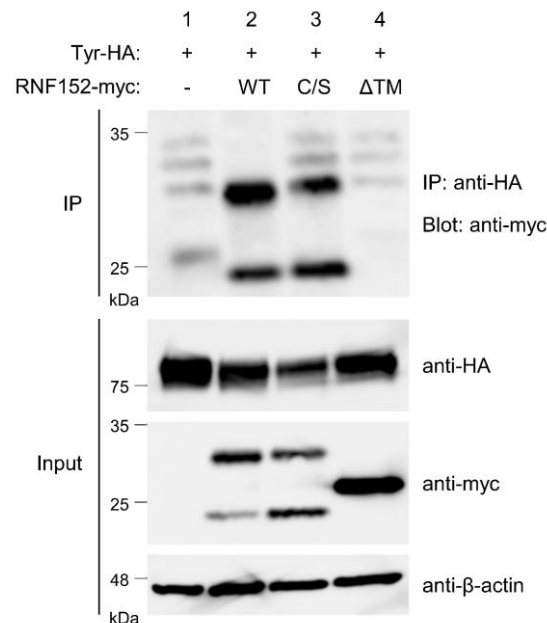
Figure 4. Interaction of RNF152 with tyrosinase. Lysates of HEK293T cells transfected with tyrosinase-HA (Tyr-HA) with an empty vector (lane 1), WT RNF152-myc (lane 2), C/S mutant RNF152-myc (lane 3), or ΔTM mutant (lane 4) were immunoblotted with anti-HA, anti-myc, or anti-β-actin antibody. Lysates were also immunoprecipitated with anti-HA antibodies, and immune complexes were immunoblotted with anti-myc antibody.

3.6. Both RING Domain and TM Domain of RNF152 are Responsible for Tyrosinase Ubiquitination

To assess the roles of the RING and TM domains of RNF152 in tyrosinase ubiquitination, we conducted a high-sensitivity ubiquitin assay using a 3×FLAG-ubiquitin plasmid in HEK293T cells. Cotransfection of tyrosinase-HA and 3×FLAG-ubiquitin with either WT or mutant RNF152-myc was performed. Blotting of total cell lysate with anti-FLAG antibody revealed a significant enhancement the ubiquitination state of any substrate proteins for WT RNF152, as evidenced by smear bands or ladder bands (Figure 5A, anti-FLAG, compare lane 1 with lane 2). In contrast, their ubiquitination state was marginally reduced in the presence of the C/S mutant and remained unaffected by the ΔTM mutant (Figure 5A, anti-FLAG, compare lane 2 with lanes 3 and 4). Immunoprecipitation of tyrosinase-HA from the cell lysate using anti-HA antibody, followed by immunoblotting with anti-FLAG antibody revealed notably enhanced smear bands, signifying strongly ubiquitinated tyrosinase for WT RNF152, whereas smear bands were faint for the C/S mutant and absent for the ΔTM mutant (Figure 5B, compare lane 2 with lanes 3 and 4).
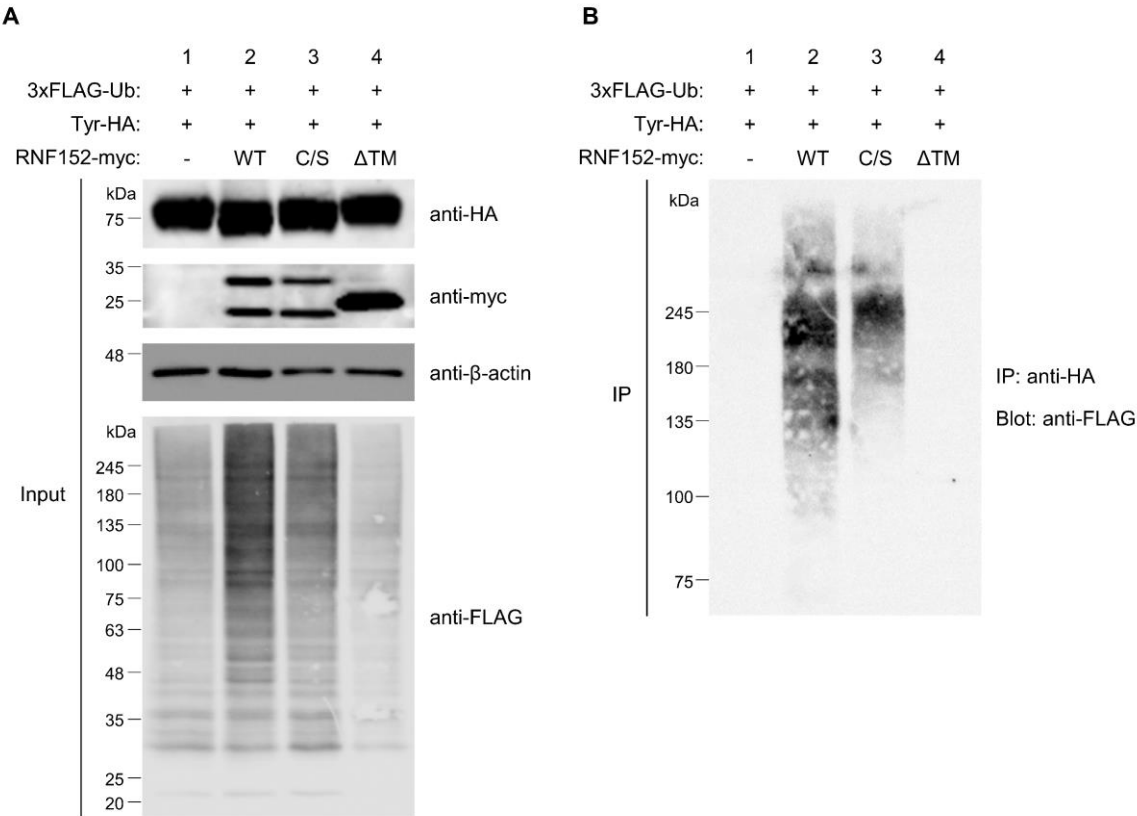
Figure 5. Tyrosinase ubiquitination by RNF152. (**A**) Lysates from HEK293T cells transfected with 3xFLAG-ubiquitin (Ub) and tyrosinase-HA (Tyr-HA) with empty vector (lane 1), WT RNF152-myc (2), C/S mutant (lane 3), or ΔTM mutant (lane 4) were immunoblotted with anti-HA, anti-myc, anti-β-actin, or anti-FLAG antibodies. (**B**) Lysates were immunoprecipitated with the anti-HA antibody, and immune complexes were immunoblotted with the anti-FLAG antibody.

3.7. Tyrp-1 Ubiquitination with RNF152

Initial observations in B16 cells did not reveal Tyrp-1 ubiquitination (Figure 1A). We further explored the potential interaction of exogenously expressed RNF152-myc with and its ubiquitination of Tyrp-1-HA (Figure 6A–C). Co-IP analysis showed that RNF152-myc interacted with Tyrp-1-HA to a similar extent as with tyrosinase-HA (Figure 6A, compare lane 2 with lanes 3 in IP). Using a high-sensitivity ubiquitination assay with 3×FLAG-ubiquitin, we observed that RNF152-myc enhanced Tyrp-1-HA ubiquitination, albeit to a lesser degree than tyrosinase-HA ubiquitination (Figure 6C, compare lane 2 with lanes 3).
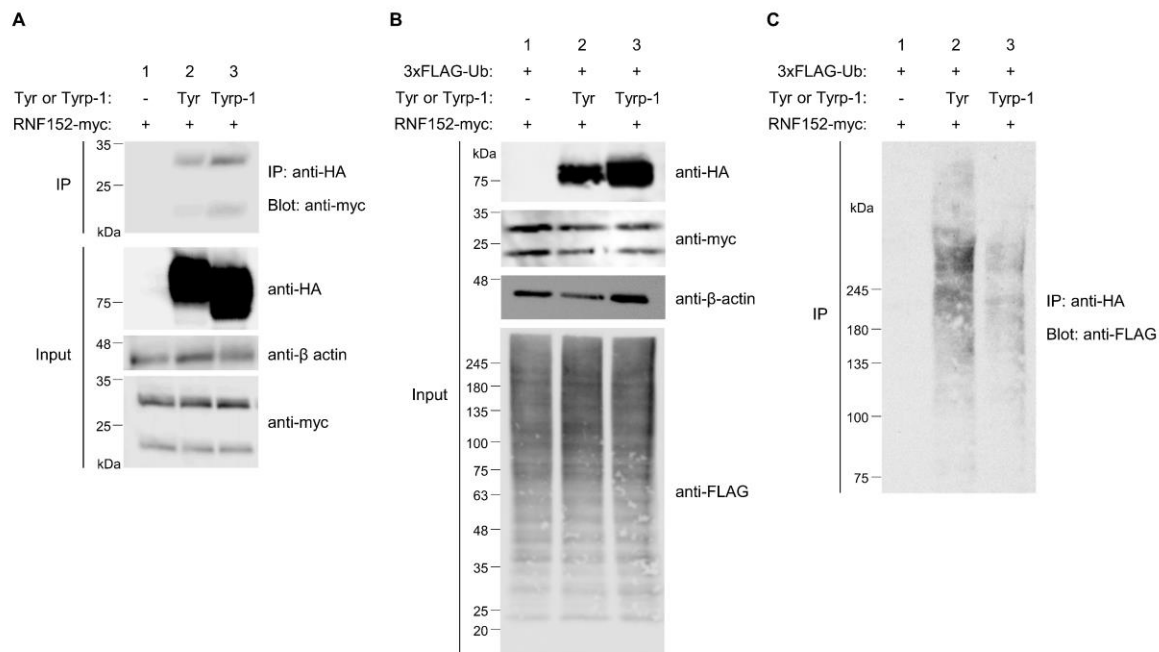
Figure 6. Ubiquitination of tyrosinase and Tyrp-1 by RNF152. (**A**) Lysates from HEK293T cells transfected with RNF152-myc with an empty vector (lane 1), tyrosinase-HA (Tyr-HA) (lane 2), or Tyrp-1-HA (lane 3) were immunoblotted with anti-HA, anti-myc, or anti-β-actin, antibodies. Lysates were also immunoprecipitated with the anti-HA antibody, and immune complexes were immunoblotted with anti-myc antibody. (**B**) Lysates from HEK293T cells transfected with 3xFLAG-ubiquitin and RNF152-myc with an empty vector (lane 1), Tyr-HA (lane 2), or Tyrp-1-HA (lane 3) were immunoblotted with anti-HA, anti-myc, anti-β-actin, or anti-FLAG antibody. (**C**) Lysates were processed as in Figure 5B.

4. Discussion

Lysosomal degradation and ubiquitination of tyrosinase have been described in numerous studies [21–25], but specific ubiquitin ligase(s) for tyrosinase have not been identified [33]. We here demonstrate that tyrosinase (but not Tyrp-1) in B16 melanoma cells undergoes ubiquitination and subsequent degradation in lysosomes. The degree of tyrosinase ubiquitination is specifically altered by both inulavosin and PTU. We hypothesized the existence of tyrosinase-specific ubiquitin ligase(s) in melanocytes that regulate tyrosinase turnover and cell pigmentation. By performing in vitro screening analysis, we identified a membrane-associated ubiquitin ligase termed RNF152, which specifically interacts with and ubiquitinates tyrosinase. In B16 cells, the expression levels of RNF152 were inversely correlated with those of tyrosinase. Given that tyrosinase level directly influences melanin content, these findings strongly suggest that RNF152 plays a pivotal role in the regulation of melanogenesis in melanocytes. In cells lacking melanosomes, such as HeLa cells, exogenously expressed tyrosinase localizes in lysosomes [34–36]. RNF152 is primarily localized in LEs and lysosomes, where it undergoes self-ubiquitination, leading to its rapid degradation due to lysosomal processes [11,37]. Upon co-expression of RNF152-myc and tyrosinase-HA, we observed their predominant localization in the TGN. However, in the presence of lysosomal inhibitors, we found them in both LEs and lysosomes. It seems likely that RNF152-myc interacts with tyrosinase-HA, ubiquitinates both itself and tyrosinase in the TGN. Subsequently, these ubiquitinated molecules might be directed to intraluminal vesicles of MVBs and degraded by lysosomal proteases. Given that self-ubiquitinated RNF152 necessitates ESCRT (Endosomal Sorting Complex Required for Transport) for its transport to intraluminal vesicles of MVBs [37], exploring whether ubiquitinated tyrosinase utilizes this ESCRT-dependent pathway is warranted. Both the RING and TM domains of RNF152 are essential for effective tyrosinase ubiquitination. The ubiquitination capability was lost in the RNF152(ΔTM) mutant but retained in the RNF152(C/S) mutant, indicating that apart from the RING domain, RNF152 likely harbors another binding site for E2

ubiquitin-conjugating enzyme(s). Conversely, the ΔTM mutant lost its ubiquitination ability due to its inability to interact with tyrosinase. Similar observations were previously reported regarding RNF152 self-ubiquitination and its role in inducing apoptosis [11,37]. Hence, the functional role of RNF152 evidently relies on subcellular localization and the TM-domain-dependent recognition of substrates. In conclusion, the ubiquitination of membrane proteins typically occurs at lysine residues located in the cytoplasmic region. Figure 7 illustrates schematic structures of tyrosinase, RNF152, and Tyrp-1 in a membrane model, along with a comparative amino acid sequences of the cytoplasmic tails of mouse tyrosinase versus mouse Tyrp-1. The cytoplasmic tail of mouse tyrosinase contains seven lysine residues, whereas that of mouse Tyrp-1 has only one. This distinction might explain why RNF152, despite its interaction with Tyrp-1, cannot efficiently ubiquitinate Tyrp-1. RNF152 evidently regulates tyrosinase protein turnover primarily through its ubiquitination activity, thereby modulating cell pigmentation by controlling the expression level of tyrosinase, a pivotal enzyme in melanin synthesis among melanocytes. Thus, compounds or factors that augment the expression levels of ubiquitin ligase(s) targeting tyrosinase as substrate, similar to RNF152, hold potential as innovative whitening reagents [38].
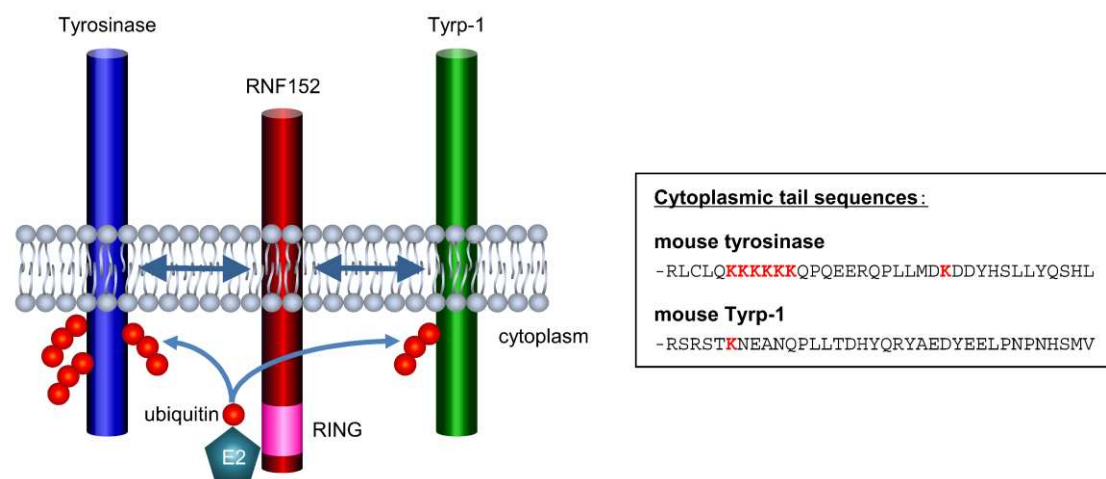
Figure 7. Proposed mechanism of RNF152 interaction and ubiquitination of tyrosinase and Tyrp-1 (schematic). The TM domain of RNF152 interacts with the TM domains of tyrosinase and Tyrp-1. In addition, RNF152 interacts with an unknown E2 ubiquitin-conjugating enzyme, and the E2 conjugates ubiquitin to lysine residue(s) of CT domains of tyrosinase and Tyrp-1. Tyrosinase undergoes stronger ubiquitination than Tyrp-1, likely due to the cytoplasmic tail of mouse tyrosinase harboring seven lysine residues, whereas that of mouse Tyrp-1 has only one.

Supplementary Materials: The following supporting information can be downloaded at the website of this paper posted on Preprints.org., Supplementary Figure S1

Acknowledgments: We thank S. Ozono (National Institute of Infectious Diseases, Japan) for technical assistance. This study was supported by grants from the Japan Society for the Promotion of Science KAKENHI Grant in-Aid for Scientific Research 21K07060 (to K.T.) and 26460086 and 21K06556 (to H.F.), the Tokyo Biochemical Research Foundation (to H.F. and J.C.J.M.D.S.M.) and Japanese Society for Pigment Cell Research (to H.F.). The authors are grateful to K. Furuta (National Cancer Center Research Institute, Tokyo) for providing mouse anti-human Lamp-1 monoclonal antibody 1D4B, and to Dr. S. Anderson for English editing of the manuscript.

Conflicts of Interest: The authors declare that they have no competing financial interests or personal relationships that could potentially influence the studies or findings described in this paper.

Abbreviations

ERAD: ER-associated degradation; IP, immunoprecipitation; LEs, late endosomes; LPIs, lysosomal protease inhibitors; MVB, multivesicular body; PTU, phenylthiourea; RING, really interesting new gene; RNF, RING finger; TGN, trans-Golgi network; TM, transmembrane; Tyrp-1, tyrosinase related protein-1.

References

1. Lecker, S.H.; Goldberg, A.L.; Mitch, W.E. Protein degradation by the ubiquitin-proteasome pathway in normal and disease states. *J Am Soc Nephrol* **2006**, *17*, 1807-1819, doi:10.1681/ASN.2006010083.
2. Apaja, P.M.; Lukacs, G.L. Protein homeostasis at the plasma membrane. *Physiology (Bethesda)* **2014**, *29*, 265-277, doi:10.1152/physiol.00058.2013.
3. Wu, X.; Rapoport, T.A. Mechanistic insights into ER-associated protein degradation. *Curr Opin Cell Biol* **2018**, *53*, 22-28, doi:10.1016/j.ceb.2018.04.004.
4. Piper, R.C.; Luzio, J.P. Ubiquitin-dependent sorting of integral membrane proteins for degradation in lysosomes. *Curr Opin Cell Biol* **2007**, *19*, 459-465, doi:10.1016/j.ceb.2007.07.002.
5. Piper, R.C.; Dikic, I.; Lukacs, G.L. Ubiquitin-dependent sorting in endocytosis. *Cold Spring Harb Perspect Biol* **2014**, *6*, doi:10.1101/cshperspect.a016808.
6. d'Azzo, A.; Bongiovanni, A.; Nastasi, T. E3 ubiquitin ligases as regulators of membrane protein trafficking and degradation. *Traffic (Copenhagen, Denmark)* **2005**, *6*, 429-441, doi:10.1111/j.1600-0854.2005.00294.x.
7. Bartee, E.; Mansouri, M.; Hovey Nerenberg, B.T.; Gouveia, K.; Fruh, K. Downregulation of major histocompatibility complex class I by human ubiquitin ligases related to viral immune evasion proteins. *Journal of virology* **2004**, *78*, 1109-1120.
8. Fujita, H.; Iwabu, Y.; Tokunaga, K.; Tanaka, Y. Membrane-associated RING-CH (MARCH) 8 mediates the ubiquitination and lysosomal degradation of the transferrin receptor. *Journal of cell science* **2013**, *126*, 2798-2809, doi:10.1242/jcs.119909.
9. Fukuda, H.; Nakamura, N.; Hirose, S. MARCH-III Is a novel component of endosomes with properties similar to those of MARCH-II. *Journal of biochemistry* **2006**, *139*, 137-145, doi:10.1093/jb/mvj012.
10. Tada, T.; Zhang, Y.; Fujita, H.; Tokunaga, K. MARCH8: the tie that binds to viruses. *FEBS J* **2022**, *289*, 3642-3654, doi:10.1111/febs.16017.
11. Zhang, S.; Wu, W.; Wu, Y.; Zheng, J.; Suo, T.; Tang, H.; Tang, J. RNF152, a novel lysosome localized E3 ligase with pro-apoptotic activities. *Protein & cell* **2010**, *1*, 656-663, doi:10.1007/s13238-010-0083-1.
12. Deng, L.; Jiang, C.; Chen, L.; Jin, J.; Wei, J.; Zhao, L.; Chen, M.; Pan, W.; Xu, Y.; Chu, H.; et al. The ubiquitination of rag A GTPase by RNF152 negatively regulates mTORC1 activation. *Molecular cell* **2015**, *58*, 804-818, doi:10.1016/j.molcel.2015.03.033.
13. Okamoto, T.; Imaizumi, K.; Kaneko, M. The Role of Tissue-Specific Ubiquitin Ligases, RNF183, RNF186, RNF182 and RNF152, in Disease and Biological Function. *Int J Mol Sci* **2020**, *21*, doi:10.3390/ijms21113921.
14. Jimbow, K.; Gomez, P.F.; Toyofuku, K.; Chang, D.; Miura, S.; Tsujiya, H.; Park, J.S. Biological role of tyrosinase related protein and its biosynthesis and transport from TGN to stage I melanosome, late endosome, through gene transfection study. *Pigment cell research* **1997**, *10*, 206-213.
15. Marks, M.S.; Seabra, M.C. The melanosome: membrane dynamics in black and white. *Nature reviews. Molecular cell biology* **2001**, *2*, 738-748, doi:10.1038/35096009.
16. Orlow, S.J.; Boissy, R.E.; Moran, D.J.; Pifko-Hirst, S. Subcellular distribution of tyrosinase and tyrosinase-related protein-1: implications for melanosomal biogenesis. *The Journal of investigative dermatology* **1993**, *100*, 55-64.
17. Raposo, G.; Marks, M.S. The dark side of lysosome-related organelles: specialization of the endocytic pathway for melanosome biogenesis. *Traffic (Copenhagen, Denmark)* **2002**, *3*, 237-248.
18. Raposo, G.; Tenza, D.; Murphy, D.M.; Berson, J.F.; Marks, M.S. Distinct protein sorting and localization to premelanosomes, melanosomes, and lysosomes in pigmented melanocytic cells. *The Journal of cell biology* **2001**, *152*, 809-824.
19. Wang, N.; Hebert, D.N. Tyrosinase maturation through the mammalian secretory pathway: bringing color to life. *Pigment cell research* **2006**, *19*, 3-18, doi:10.1111/j.1600-0749.2005.00288.x.
20. Solano, F.; Briganti, S.; Picardo, M.; Ghanem, G. Hypopigmenting agents: an updated review on biological, chemical and clinical aspects. *Pigment cell research* **2006**, *19*, 550-571, doi:10.1111/j.1600-0749.2006.00334.x.
21. Ando, H.; Watabe, H.; Valencia, J.C.; Yasumoto, K.; Furumura, M.; Funasaka, Y.; Oka, M.; Ichihashi, M.; Hearing, V.J. Fatty acids regulate pigmentation via proteasomal degradation of tyrosinase: a new aspect of ubiquitin-proteasome function. *The Journal of biological chemistry* **2004**, *279*, 15427-15433, doi:10.1074/jbc.M313701200.
22. Ando, H.; Wen, Z.M.; Kim, H.Y.; Valencia, J.C.; Costin, G.E.; Watabe, H.; Yasumoto, K.; Niki, Y.; Kondoh, H.; Ichihashi, M.; et al. Intracellular composition of fatty acid affects the processing and function of

tyrosinase through the ubiquitin-proteasome pathway. *The Biochemical journal* **2006**, *394*, 43-50, doi:10.1042/bj20051419.

23. Hall, A.M.; Orlow, S.J. Degradation of tyrosinase induced by phenylthiourea occurs following Golgi maturation. *Pigment cell research* **2005**, *18*, 122-129, doi:10.1111/j.1600-0749.2005.00213.x.

24. Fujita, H.; Motokawa, T.; Katagiri, T.; Yokota, S.; Yamamoto, A.; Himeno, M.; Tanaka, Y. Inulavosin, a melanogenesis inhibitor, leads to mistargeting of tyrosinase to lysosomes and accelerates its degradation. *The Journal of investigative dermatology* **2009**, *129*, 1489-1499, doi:10.1038/jid.2008.376.

25. Fujita, H.; Menezes, J.C.; Santos, S.M.; Yokota, S.; Kamat, S.P.; Cavaleiro, J.A.; Motokawa, T.; Kato, T.; Mochizuki, M.; Fujiwara, T.; et al. Inulavosin and its benzo-derivatives, melanogenesis inhibitors, target the copper loading mechanism to the active site of tyrosinase. *Pigment cell & melanoma research* **2014**, *27*, 376-386, doi:10.1111/pcmr.12225.

26. Fujita, H.; Sasano, E.; Yasunaga, K.; Furuta, K.; Yokota, S.; Wada, I.; Himeno, M. Evidence for distinct membrane traffic pathways to melanosomes and lysosomes in melanocytes. *The journal of investigative dermatology. Symposium proceedings* **2001**, *6*, 19-24, doi:10.1046/j.0022-202x.2001.00009.x.

27. Sawasaki, T.; Kamura, N.; Matsunaga, S.; Saeki, M.; Tsuchimochi, M.; Morishita, R.; Endo, Y. Arabidopsis HY5 protein functions as a DNA-binding tag for purification and functional immobilization of proteins on agarose/DNA microplate. *FEBS letters* **2008**, *582*, 221-228, doi:10.1016/j.febslet.2007.12.004.

28. Sawasaki, T.; Ogasawara, T.; Morishita, R.; Endo, Y. A cell-free protein synthesis system for high-throughput proteomics. *Proc Natl Acad Sci U S A* **2002**, *99*, 14652-14657, doi:10.1073/pnas.232580399.

29. Takahashi, H.; Uematsu, A.; Yamanaka, S.; Imamura, M.; Nakajima, T.; Doi, K.; Yasuoka, S.; Takahashi, C.; Takeda, H.; Sawasaki, T. Establishment of a Wheat Cell-Free Synthesized Protein Array Containing 250 Human and Mouse E3 Ubiquitin Ligases to Identify Novel Interaction between E3 Ligases and Substrate Proteins. *PloS one* **2016**, *11*, e0156718, doi:10.1371/journal.pone.0156718.

30. Kim, D.S.; Kim, S.Y.; Park, S.H.; Choi, Y.G.; Kwon, S.B.; Kim, M.K.; Na, J.I.; Youn, S.W.; Park, K.C. Inhibitory effects of 4-n-butylresorcinol on tyrosinase activity and melanin synthesis. *Biological & pharmaceutical bulletin* **2005**, *28*, 2216-2219, doi:10.1248/bpb.28.2216.

31. Tachiyama, R.; Ishikawa, D.; Matsumoto, M.; Nakayama, K.I.; Yoshimori, T.; Yokota, S.; Himeno, M.; Tanaka, Y.; Fujita, H. Proteome of ubiquitin/MVB pathway: possible involvement of iron-induced ubiquitylation of transferrin receptor in lysosomal degradation. *Genes to cells: devoted to molecular & cellular mechanisms* **2011**, *16*, 448-466, doi:10.1111/j.1365-2443.2011.01499.x.

32. Yurkow, E.J.; Laskin, J.D. Purification of tyrosinase to homogeneity based on its resistance to sodium dodecyl sulfate-proteinase K digestion. *Arch Biochem Biophys* **1989**, *275*, 122-129, doi:10.1016/0003-9861(89)90356-1.

33. Allouche, J.; Rachmin, I.; Adhikari, K.; Pardo, L.M.; Lee, J.H.; McConnell, A.M.; Kato, S.; Fan, S.; Kawakami, A.; Suita, Y.; et al. NNT mediates redox-dependent pigmentation via a UVB- and MITF-independent mechanism. *Cell* **2021**, *184*, 4268-4283 e4220, doi:10.1016/j.cell.2021.06.022.

34. Winder, A.J.; Wittbjer, A.; Rosengren, E.; Rorsman, H. The mouse brown (b) locus protein has dopachrome tautomerase activity and is located in lysosomes in transfected fibroblasts. *Journal of cell science* **1993**, *106 (Pt 1)*, 153-166.

35. Calvo, P.A.; Frank, D.W.; Bieler, B.M.; Berson, J.F.; Marks, M.S. A cytoplasmic sequence in human tyrosinase defines a second class of di-leucine-based sorting signals for late endosomal and lysosomal delivery. *The Journal of biological chemistry* **1999**, *274*, 12780-12789.

36. Simmen, T.; Schmidt, A.; Hunziker, W.; Beermann, F. The tyrosinase tail mediates sorting to the lysosomal compartment in MDCK cells via a di-leucine and a tyrosine-based signal. *Journal of cell science* **1999**, *112 (Pt 1)*, 45-53.

37. Zhang, W.; Yang, X.; Chen, L.; Liu, Y.Y.; Venkatarangan, V.; Reist, L.; Hanson, P.; Xu, H.; Wang, Y.; Li, M. A conserved ubiquitin- and ESCRT-dependent pathway internalizes human lysosomal membrane proteins for degradation. *PLoS Biol* **2021**, *19*, e3001361, doi:10.1371/journal.pbio.3001361.

38. Shi, J.; Guo, Y.; Wang, H.; Xiao, Y.; Liu, W.; Lyu, L. The ubiquitin-proteasome system in melanin metabolism. *J Cosmet Dermatol* **2022**, *21*, 6661-6668, doi:10.1111/jocd.15433.